Heliyon 10 (2024) e40966

Contents lists available at ScienceDirect

Heliyon

journal homepage: www.cell.com/heliyon

Research article

Overexpression of C1orf74 predicts poor outcome and promote cervical cancer progression

Hai Zhu [a], Yaping Wang [a,b], Yu Zhang [a], Yun Tian [a,b], Duan Liu [a], Xiabing Li [a], Gaili Ji [b,c], Caixia Ma [b,c], Hongyu Li [a,b,*]

[a] Gynecologic Oncology, The Third Affiliated Hospital of Zhengzhou University, Zhengzhou, 450052, Henan, China
[b] Zhengzhou Key Laboratory of Gynecological Oncology, Zhengzhou, 450052, Henan, China
[c] Department of Gynecology and Obstetrics, The Third Affiliated Hospital, Zhengzhou University, Zhengzhou, 450052, China

ARTICLE INFO

Keywords:
C1orf74
Cervical cancer
Prognosis
Immune infiltration
Immune checkpoints

ABSTRACT

Cervical cancer (CC), which ranks among the four most common cancers in women, is a leading cause of both illness and death globally. It's urgent to identify a new biomarker to elucidate the potential mechanisms underlying the progression of CC. Here, we screened the differentially expressed genes (DEGs) in the Cancer Genome Atlas database (TCGA) and selected Chromosome 1 open reading frame 74 (C1orf74) for further investigation. C1orf74 levels were elevated, indicating a link to poor prognosis.

Higher expression of C1orf74 was significantly related to clinical stage, T stage, histological type and survival status. Functional enrichment analysis indicated that C1orf74 is likely associated with the MAPK signaling pathway. Moreover, we found that C1orf74 was correlated with multifarious immune cell infiltration. Finally, the knockdown of C1orf74 significantly inhibited the growth of CC in vitro. In conclusion, C1orf74 promotes CC proliferation and progression, is closely associated with poor prognosis, and plays a role in the tumor immune microenvironment. The research indicates that C1orf74 is important for treating CC and may help develop new strategies to improve patient outcomes.

1. Introduction

Cervical cancer (CC) is a gynecological malignant tumor with the highest incidence in women of childbearing age [1]. According to 2020 global statistics, it is one of the most commonly diagnosed cancers among the four gynecological malignancies and the fourth major cause of cancer-related death in women [2]. Despite advancements in surgery, chemotherapy, and radiotherapy, the recurrence rate and metastasis rate of advanced cervical cancer remain high at 40.3 % and 31 %, respectively [3]. The median survival for patients with advanced cervical cancer is merely 8–13 months [4], and the prognosis remains be poor. Consequently, there is of great importance for explore effective predictive biomarkers and molecular mechanisms involved in the prognosis of cervical cancer, which may play a crucial role in the discovery of better predictive and therapeutic targets.

The protein C1ORF74 encoded by the C1orf74 gene located in the chromosomal position of 1q32.2. It has been confirmed that C1orf74 is up-regulated in lung adenocarcinoma and the higher the expression, the worse the prognosis. High expression of C1orf74

* Corresponding author. Gynecologic Oncology, The Third Affiliated Hospital of Zhengzhou University, No. 7 Kangfu Front Street, Zhengzhou, Henan, 450000, China.
E-mail address: lihongyu99@zzu.edu.cn (H. Li).

https://doi.org/10.1016/j.heliyon.2024.e40966
Received 2 September 2024; Received in revised form 1 November 2024; Accepted 4 December 2024
Available online 9 December 2024

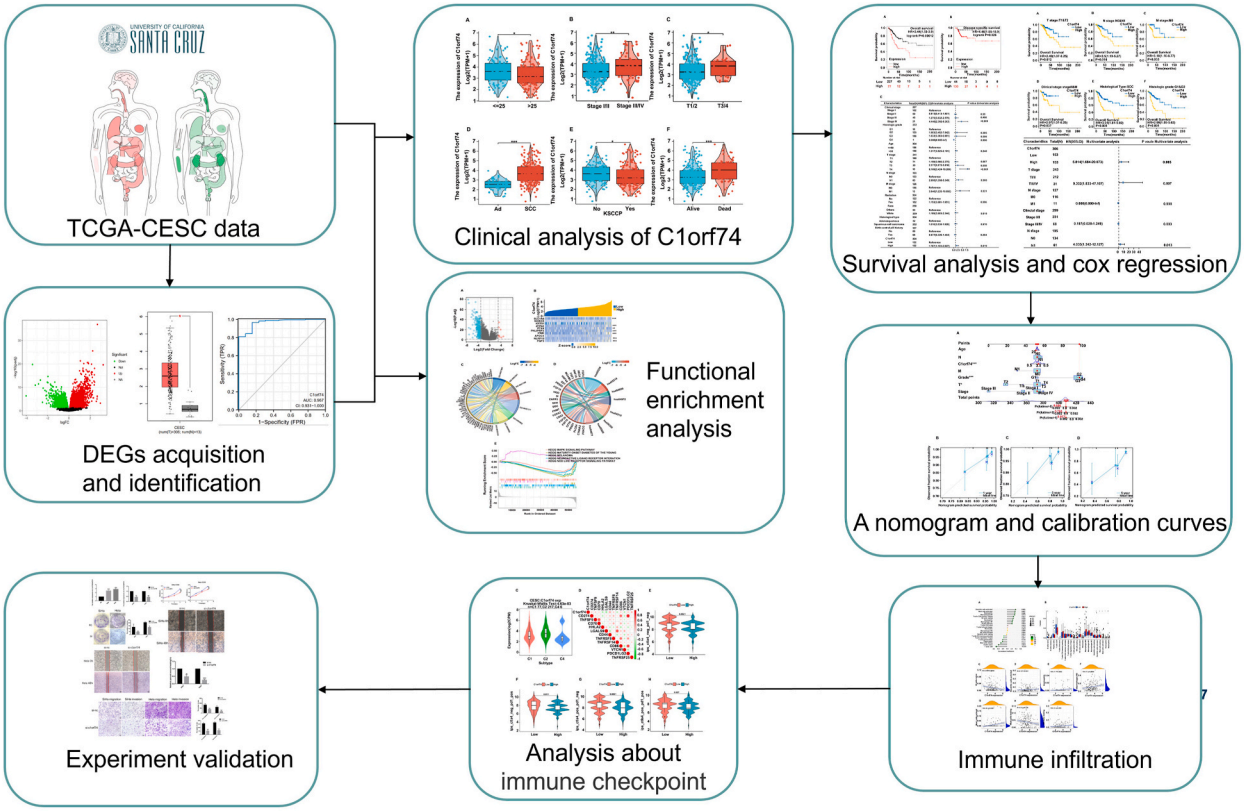

Fig. 1. Flow chart of this study.

can promote the proliferation and mobility of lung adenocarcinoma cells through the EGFR/AKT/mTORC1 signaling pathway [5]. Wang et al. found that C1orf74 may be involved in blood glucose metabolism in 2020 [6]. In addition, Guo et al. found that highly expressed C1orf74 and neutrophils are closely related to poor prognosis in CC patients, and may serve as potential biomarkers for cervical cancer prognosis in 2022 [7]. The role of C1orf74 in CC has not been reported.

Using data from The Cancer Genome Atlas (TCGA), this investigation aimed to elucidate the association between C1orf74 expression and its impact on the malignant biological characteristics of CC cells, alongside its relationship with clinicopathological parameters, prognostic relevance, and immune cell infiltration. The expression levels of C1orf74 were assessed in CC tissue samples and cell lines through quantitative reverse transcription polymerase chain reaction (qRT-PCR) analysis. To evaluate the potential roles of C1orf74 in the proliferation, migration, and invasion of cervical cancer cells, various assays including transwell, wound healing, CCK-8, and colony formation were employed. Collectively, our results may assist clinical application specialists in enhancing treatment strategies and optimizing outcomes for patients diagnosed with CC. The overall methodology of this study is illustrated in Fig. 1. This study was approved by the Third Affiliated Hospital of Zhengzhou University's medical ethics committee (ethics approval number: 2024-362-01).

2. Materials and method

2.1. Data collection analysis

The mRNA expression profiles, along with the associated clinicopathological information for cervical squamous cell carcinoma and endocervical adenocarcinoma (CESC), were obtained from the TCGA database [8] (https://portal.gdc.cancer.gov/) and the Genotype Tissue Expression Project (GTEx) database [9] (https://commonfund.nih.gov/gtex). Data formatted as transcripts per million reads (TPM) were sourced from both the UCSC Xena database [10] (https://xenabrowser.net/datapages/) and the GTEx database.

2.2. Identification of differentially expressed genes (DEGs)

Initially, data encompassing survival duration and clinical characteristics were obtained, which included samples from 3 normal cervical tissues and 306 cervical cancer tissues. Subsequently, the genes that exhibited upregulation in cervical cancer tissues relative to normal tissues were identified using the limma package in R, applying the criteria of |log-fold-change (FC)|>1 and $p < 0.05$ after

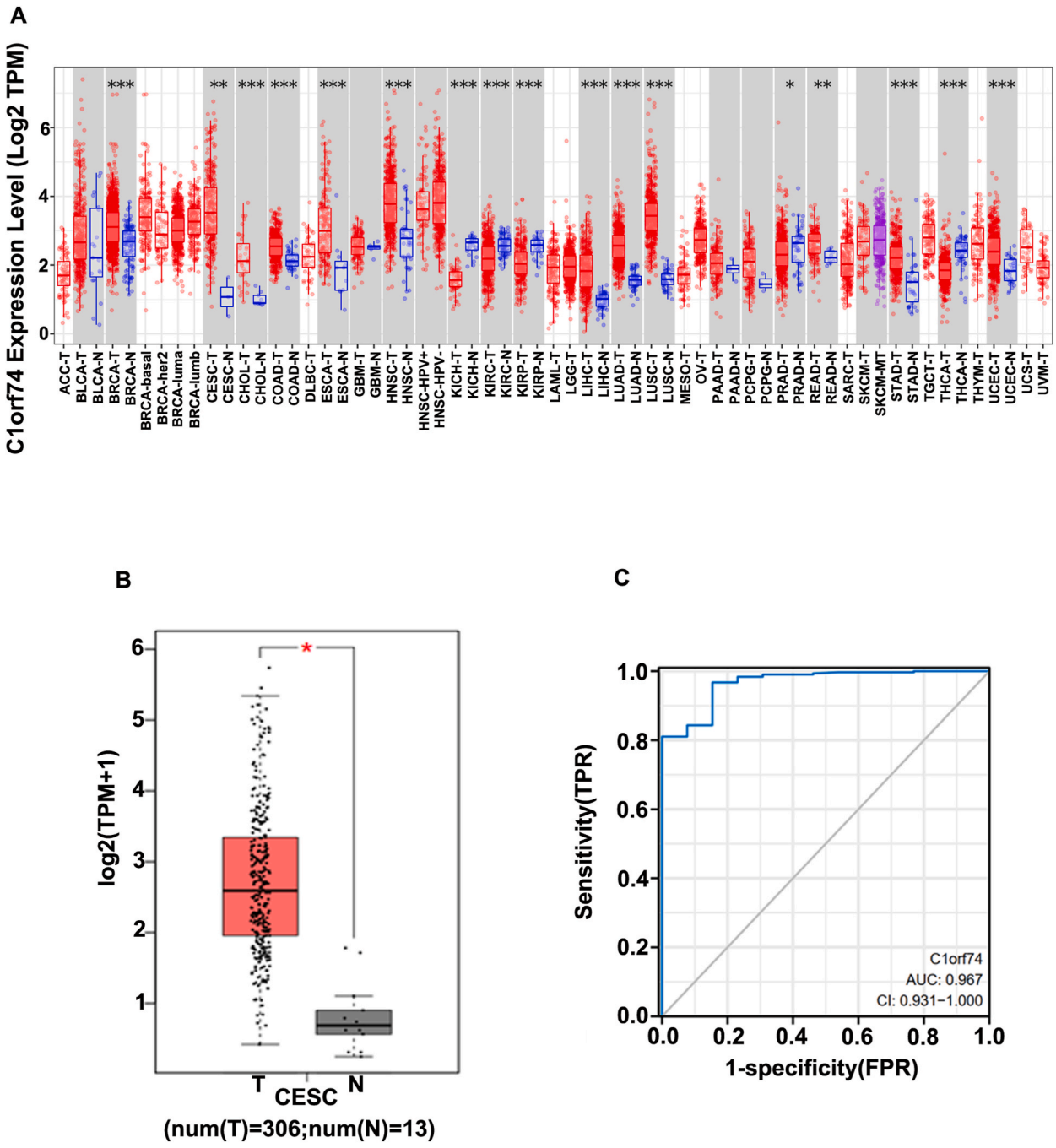

Fig. 2. Expression levels of C1orf74 in different types of tumors and cervical cancer. Expression of C1orf74 **(A)** in different types of tumors compared with normal tissues in TCGA and GTEx databases. **(B)** In cervical cancer and non-matched normal tissues in the TCGA and GTEx databases. **(C)** ROC curves for classifying cervical cancer versus normal cervical tissues in the TCGA database. TCGA, The Cancer Genome Atlas; GTEx, Genotype Tissue Expression Project; T, tumor; N, normal tissue; ROC, receiver operating characteristic. *, $p < 0.05$; **, $p < 0.01$; and ***, $p < 0.001$.

processing the TCGA data [11]. In the next step, the upregulated differentially expressed genes (DEGs) underwent analysis through the Kaplan-Meier (KM) method and the single-gene Cox regression method, with both methods adhering to a significance threshold of $p < 0.05$. To determine whether the identified genes could serve as independent prognostic indicators, we used the criteria of hazard ratio (HR) > 1 and $p < 0.05$, along with an area under the curve (AUC$>$0.60) to filter genes related to clinical staging. Ultimately, two genes, C1orf74 and PGK1 (phosphoglycerate kinase), were identified as being linked to clinical stage, with PGK1 having been previously reported in the context of cervical cancer [12], therefore, this investigation focus on C1orf74. Following this, we examined the

Table 1
Association between C1orf74 expression and clinicopathological characteristics of in patients with cervical cancer in TCGA.

Characteristics	Total	C1orf74 expression		X^2	p Value
	N	Low	High		
T stage				7.589	**0.006****
T1/T2	211	114	97		
T3/T4	30	10	20		
Others	63	–	–		
N stage				0.783	0.376
N0	133	69	64		
N1	60	27	33		
Others	111	–	–		
M stage					0.749[a]
M0	116	61	55		
M1	10	6	4		
Others	178	–	–		
Clinical stage				12.945	**<0.001*****
Stage I/II	231	128	103		
Stage III/IV	56	20	46		
Others	17	–	–		
Radiation therapy				0.055	0.815
No	122	60	62		
Yes	182	92	90		
Primary therapy outcome				0.033	0.855
PD/SD	28	14	14		
PR/CR	189	98	91		
Others	87	–	–		
Weight				6.114	**0.013***
≤70	138	59	79		
>70	137	79	58		
Others	29	–	–		
Height				0.032	0.859
≤160	133	69	64		
>160	128	65	63		
Others	43	–	–		
BMI(kg/㎡)				4.548	**0.033***
≤25	100	43	57		
>25	159	90	69		
Others	45	–	–		
Histological type				53.451	**<0.001*****
Adenosquamous	52	50	2		
Squamous cell carcinoma	252	102	150		
Histologic grade				0.797	0.372
G1/2	153	74	79		
G3/4	119	63	56		
Others	32	–	–		
Menopause status				0.004	0.947
Pre	149	77	72		
Post	82	42	40		
Others	73	–	–		
KSCCP				7.305	**0.007****
No	119	48	71		
Yes	185	104	81		
OS event				8.104	**0.004*****
Alive	233	127	106		
Dead	71	25	46		

T: T stage; N0: No lymph node metastasis; N1: Lymph node metastasis; M0: No distant metastasis; M1: Distant metastasis; PD: Progressive disease; SD: Stable disease; PR: Partial response; CR: Complete response; BMI: Body mass index; G: Histologic grade; KSCCP: Keratinizing squamous cell carcinoma present; a indicates the Fisher test, and the other test was the Chi-square test; (*, $P < 0.05$; **, $P < 0.01$; ***, $P < 0.001$.).

correlation between C1orf74 expression and various clinical parameters, while also assessing the prognostic significance of C1orf74 in CC.

2.3. Survival and prognosis analysis

Survival analysis was conducted employing the Kaplan-Meier (KM) method alongside the log-rank test, with the cutoff value established at the median expression level of C1orf74. To evaluate the influence of clinical variables on patient prognosis, both univariate and multivariate Cox regression analyses were implemented. Prognostic variables that demonstrated a significance level of $p < 0.05$ in the univariate Cox regression analysis were subsequently incorporated into the multivariate Cox regression analysis. The

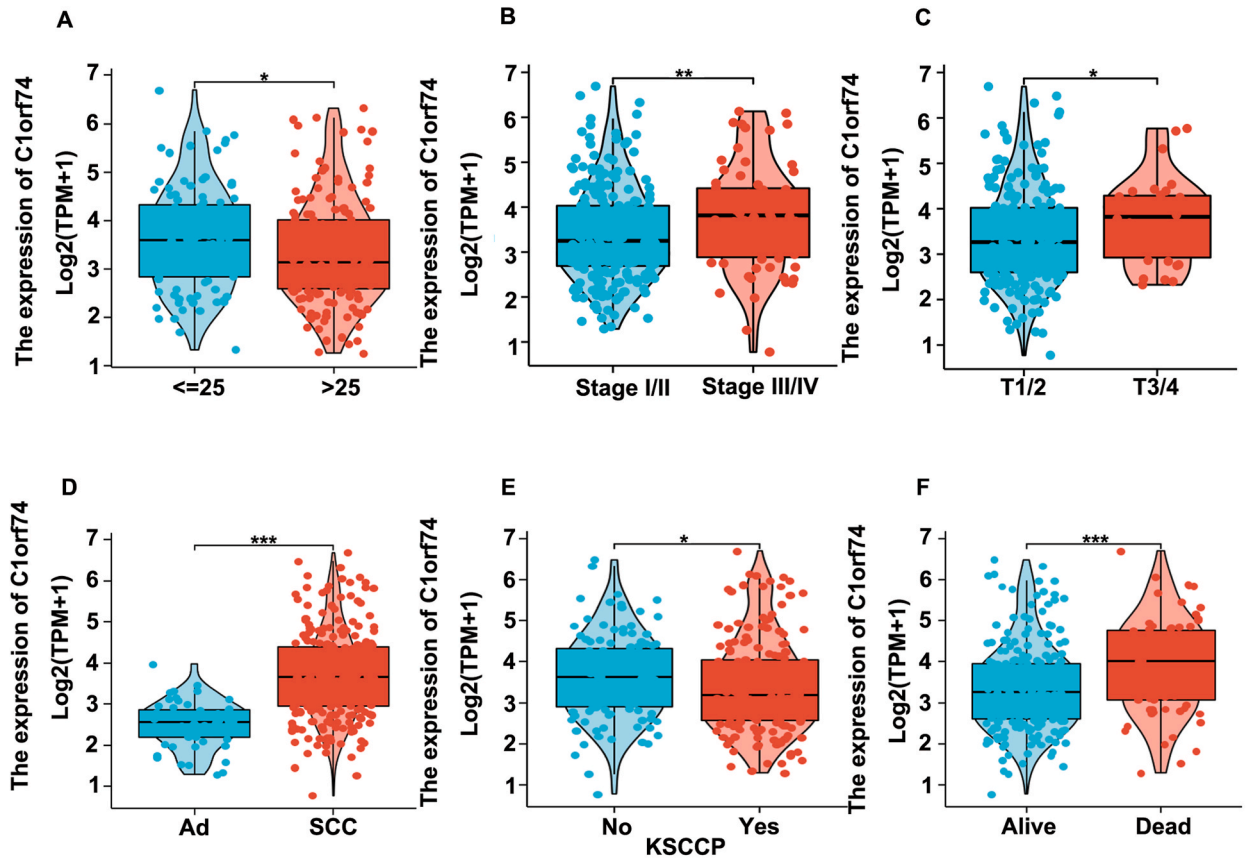

Fig. 3. Associations between C1orf74 expression and clinicopathological characteristics. Data are shown for **(A)** BMI. **(B)** Clinical stage. **(C)** T stage. **(D)** Histological type. **(E)** KSCCP. **(F)** OS event. BMI, Body mass index; KSCCP, Keratinizing squamous cell carcinoma present; OS, overall survival; Ad, adenosquamous; SCC, squamous cell carcinoma. *, $p < 0.05$; **, $p < 0.01$; and ***, $p < 0.001$.

visualization of forest plots was accomplished using the R package ggplot2.

2.4. Construction and validation of the nomogram

A nomogram was created using independent prognostic factors with the "rms" and "survivor" R packages [13]. Following this, a calibration plot was used to evaluate how well the nomogram predicts outcomes, while the concordance index (C-index) [14] assessed its ability to differentiate between groups.

2.5. Functional enrichment analysis

The analysis of DEGs aimed to identify functional enrichments using Gene Ontology (GO), Kyoto Encyclopedia of Genes and Genomes (KEGG), and Gene Set Enrichment Analysis (GSEA). This was accomplished through the application of the R package clusterProfiler, along with org.Hs.eg.db and enrichplot (version 1.0.2) [15,16]. An false discovery rate (FDR) of less than 0.25, along with an adjusted p-value of less than 0.05, were considered indicators of statistically significant enrichment in functional or pathway terms.

2.6. Immune infiltration analysis

A thorough examination was performed using 22 gene expression profiles of immune cells alongside immune cell infiltration data sourced from the TIMER database [17] (https://cistrome.shinyapps.io/timer/) to evaluate the degree of immune infiltration. The differences in immune infiltration levels between groups with high and low expression of C1orf74 were assessed using the Wilcoxon rank-sum test. Additionally, the association between C1orf74 expression and different types of immune cells was investigated through Spearman correlation analysis.

Table 2
Logistic regression model of prognostic factors in patients with cervical cancer in TCGA.

Characteristics	OR	95%CI	P Value
T stage (T3/T4 vs T1/T2)	2.351	1.072–5.462	**0.038***
N stage (N1 vs N0)	1.318	0.716–2.442	0.377
M stage (M1 vs M0)	0.739	0.181–2.724	0.653
Clinical stage (Stage III/IV vs Stage I/II)	2.858	1.611–5.224	**<0.001*****
Age (>50 vs ≤50)	0.801	0.504–1.271	0.347
Race (White vs Others)	0.731	0.388–1.358	0.325
Radiation therapy (Yes vs No)	0.947	0.598–1.498	0.815
Histological type (SCC vs AD)	36.765	11.071–227.953	**<0.001*****
Histologic grade (G3/G4 vs G1/G2)	0.833	0.515–1.345	0.454
KSCCP (Yes vs No)	0.527	0.329–0.838	**0.007****

T: T stage; N0: No lymph node metastasis; N1: Lymph node metastasis; M0: No distant metastasis; M1: Distant metastasis; G: Histologic grade; KSCCP: Keratinizing squamous cell carcinoma present; SCC: Squamous Cell Carcinoma; AD: Adenosquamous; G: Histologic grade; KSCCP: keratinizing squamous cell carcinoma present; (*, $P < 0.05$; **, $P < 0.01$; ***, $P < 0.001$.).

2.7. Immune checkpoints analysis

The immunophenoscores (IPS) related to CC were obtained from the Cancer Immunome Atlas (TCIA) database (https://tcia.at/, accessed on November 16, 2022) [18]. To predict sensitivity to immunotherapy, we investigated the association between C1orf74 and induced IPS. The Tumor Immune Dysfunction and Exclusion (TIDE) score was calculated using the TIDE algorithm (accessible at http://tide.dfci.harvard.edu/, accessed on November 16, 2022) to evaluate the patients' potential response to immune checkpoint blockade (ICB) therapy. The primary targets of ICB treatment include programmed death-ligand 1 (PD-L1), programmed cell death protein 1 (PD-1), and cytotoxic T-lymphocyte-associated protein 4 (CTLA-4) [19].

2.8. qRT-PCR

Total RNA was isolated from the cells using Trizol solution (TransGen Biotech, China) in accordance with the manufacturer's instructions. Subsequently, the RNA from each sample underwent reverse transcription using the PrimeScript RT reagent kit (TOYOBO, Japan). Quantitative real-time polymerase chain reaction (qRT-PCR) was conducted with the application of specific primers and the SYBR Green qPCR Master Mix (CWBIO, China). The specific primers used are as follows: GGAGTCCACTGGCGTCTTCA forward and GTCATGAGTCCTTCCACGATACC reverse for glyceraldehyde-3phosphate dehydrogenase (GAPDH); and TCCTGAGCATG-TATGTCAGCA forward, CCCTGCAAATGTGTGATGATCTC reverse for C1orf74 [20]. The expression levels of C1orf74 and GAPDH were assessed for each sample, with GAPDH serving as the internal control. Subsequently, the relative expression levels of C1orf74 were determined by calculating the ratio of the 2^-ΔCt value of C1orf74 to the 2^-ΔCt value of GAPDH [21].

2.9. Cell culture

The human cervical cancer cell lines SiHa and HeLa, along with the normal human cervical cell line H8, were maintained in a complete medium consisting of RPMI-1640 supplemented with 10 % fetal bovine serum (BI, USA). These cell lines were incubated at 37 °C in an environment containing 5 % CO_2.

2.10. Cell transfection

C1orf74 small interfering RNA (siRNA) (5′-GCCAGCUGUGCUCUAUGAUTT-3′) and a negative control (NC) (5′-UUCUCCGAAC-GUGUCACGUTT-3′) (GenePharma, China) were transfected into SiHa and HeLa cells according to the manufacturer's instructions. The transfection of C1orf74 siRNA and its negative controls was conducted in 6-well plates. A serum-free medium without antibodies against double-stranded RNA and the transfection reagent Lipofectamine™ 3000 (Invitrogen, USA) were used. After an incubation period of 8 h, the culture medium was replaced with 10 % fetal bovine serum. Subsequently, after a transfection period of 48 h, the cells were collected for subsequent experimental analyses.

2.11. CCK-8 assay

Cells were cultured at 37 °C in 96-well plates at a density of approximately 1×10^3 for 0, 24, 48 and 72 h. Subsequently,10 μL of CCK-8 solution (SEVEN, China) was added to each well, following the manufacturer's instructions. The optical density of each well was detected at 450 nm.

2.12. Colony formation assay

Cells in a 6-well plate with approximately 1×10^3 cells/well were cultured for 13 days. After cells were fixed and stained with

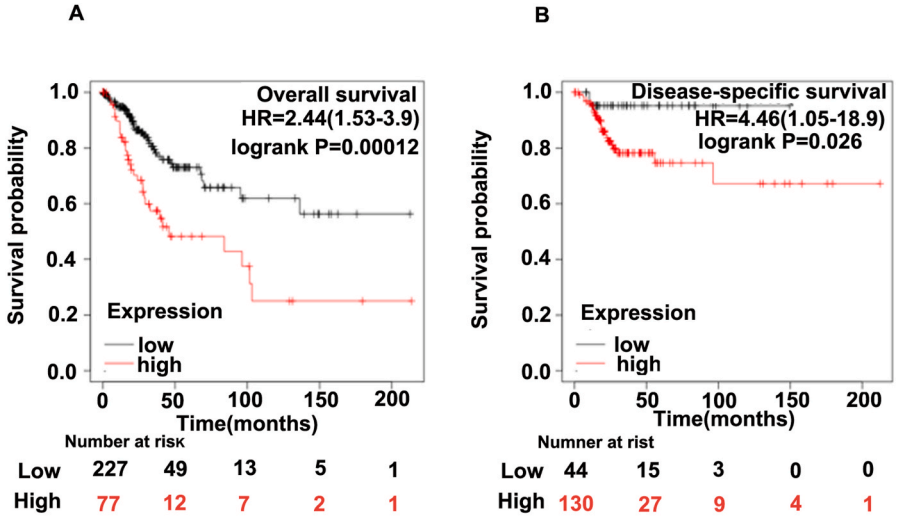

C

Characteristics	Total(N)	HR(95% CI)Univariate analysis	P value Univariate analysis
Clinical stage	297		
Stage I	162	Reference	
Stage II	69	0.813(0.413-1.601)	0.55
Stage III	45	1.275(0.632-2.570)	0.498
Stage IV	21	4.446(2.392-8.263)	<0.001
Histologic grade	272		
G1	18	Reference	
G2	135	1.883(0.452-7.842)	0.385
G3	118	1.633(0.383-6.961)	0.508
G4	1	0.000(0.000-inf)	0.996
Age	304		
<=50	186	Reference	
>50	118	1.317(0.825-2.101)	0.248
T stage	241		
T1	140	Reference	
T2	71	1.159(0.566-2.375)	0.687
T3	20	2.377(0.972-5.816)	0.058
T4	10	8.109(3.424-19.200)	<0.001
N stage	193		
N0	133	Reference	
N1	60	2.695(1.358-5.349)	0.005
M stage	126		
M0	116	Reference	
M1	10	3.646(1.220-10.892)	0.021
Radiation	304		
No	122	Reference	
Yes	182	1.153(0.681-1.951)	0.596
Race	259		
Others	50	Reference	
White	209	1.189(0.603-2.344)	0.618
Histological type	304		
Adenosquamous	52	Reference	
Squamous cell carcinoma	252	1.010(0.530-1.926)	0.976
Birth control pill history	157		
No	89	Reference	
Yes	68	0.677(0.326-1.404)	0.294
C1orf74	304		
Low	152	Reference	
High	152	1.797(1.103-2.927)	0.019

(caption on next page)

Fig. 4. Prognostic values of C1orf74 expression in patients with cervical cancer evaluated by the Kaplan-Meier method. Overall survival **(A)** and disease-specific survival **(B)** for cervical cancer patients with high versus low C1orf74. **(C)** Forest map based on univariate Cox analysis for overall survival. HR, hazard ratio; CI, confidence interval. T, T stage; N, N stage; M, M stage.

Methanol and 0.1 % crystal violet count the colonies.

2.13. Wound healing assay

When confluence reached 90 % in a 6-well plate, a 200 μl sterile pipette tip was applied to create streaks in the cell monolayers. Then the images were captured at 0 h, 24 h and 48 h under 40× magnification, and the degree of wound closure was measured with ImageJ software.

2.14. Transwell assay

The Transwell assay was employed to assess the invasive and migratory capabilities of cervical cancer cells using a 24-well Transwell chamber with an 8 μm pore size (Corning, USA). For the invasion assay, the chamber was coated with Matrigel (BD Bioscience, USA), while for the migration assay, it was uncoated. A total of 8×10^4 cells were resuspended in 200 μL of serum-free medium and subsequently placed in the upper chamber, while the lower chamber was filled with a medium supplemented with 10 % fetal bovine serum. Following a 48-h incubation period, the cells were fixed using methanol and stained with 0.1 % crystal violet. The stained cells were then captured using an inverted microscope for analysis.

2.15. Statistical analysis

Bioinformatics analyses were conducted with R (version 4.2.2) and Perl (version 5.32.1) [22]. We used the Chi-square test and Fisher's exact test to assess differences in clinicopathological factors. Additionally, a survival analysis was conducted using Kaplan-Meier (KM) analysis and the log-rank test. The statistics related to the different clinical samples were analyzed using Prism 7 (GraphPad Software Inc., La Jolla, USA). $p < 0.05$ was considered as statistically significant.

3. Results

3.1. Validation of C1orf74 expression in TCGA database

To validate the dependability and precision of the aforementioned bioinformatics analysis findings, we assessed the mRNA expression levels of C1orf74 using data from the TCGA database. As illustrated in Fig. 2A, our findings revealed that the expression of C1orf74 was significantly increased in various tumor tissues when compared to normal tissues, particularly in cervical cancer (Fig. 2B). Furthermore, the receiver-operating characteristic (ROC) curve analysis showed that C1orf74 expression effectively predicts cervical cancer tissue versus normal tissue, with an area under the curve (AUC) of 0.967 (95 % confidence interval [CI] = 0.931–1.000) (Fig. 2C).

3.2. Relationship between C1orf74 expression and clinical parameters

As shown in Table 1 and Fig. 3, a pronounced expression of C1orf74 exhibited a significant correlation with various clinical parameters, including clinical stage (stage III/IV compared to stage II/I, $p < 0.001$), T stage ($p = 0.006$), histological type ($p < 0.001$), body mass index (BMI) ($p = 0.033$), and overall survival (OS) ($p = 0.004$). Furthermore, the findings from the univariate logistic regression analyses indicated notable clinicopathological differences between cohorts with elevated and diminished levels of C1orf74 expression. These differences included T stage (odds ratio [OR] = 2.351, 95 % confidence interval [CI] = 1.072–5.462, $p = 0.038$), clinical stage (OR = 2.858, 95 % CI = 1.611–5.224, $p < 0.001$), histological type (OR = 36.765, 95 % CI = 11.071–227.953, $p < 0.001$), and the presence of keratinizing squamous cell carcinoma (KSCCP) (OR = 0.527, 95 % CI = 0.329–0.838, $p = 0.007$) as detailed in Table 2.

3.3. Prognostic value of C1orf74 in cervical cancer

The association between the expression levels of C1orf74 and the prognosis of cervical cancer patients was assessed using the KM method. The median expression level of C1orf74 served as the threshold for classification, resulting in the categorization of patients into high and low expression groups. A comparative analysis revealed that the overall survival (OS) and disease-specific survival (DSS) rates for the high C1orf74 expression cohort were significantly poorer than those observed in the low expression group (OS: hazard ratio [HR] = 2.44, 95 % confidence interval [CI] = 1.53–3.90, $p = 0.00012$; DSS: HR = 4.46, 95 % CI = 1.05–18.90, $p = 0.026$) (Fig. 4A–B). Subsequently, the prognostic implications of C1orf74 expression were further investigated across various subgroups. In the analyses of both OS and DSS, patients with high C1orf74 expression consistently showed a significantly worse prognosis across several subgroups. These including T1 and T2, N0 and N1, M0 and M1, stages II and III, squamous cell carcinoma (SCC), and grades G1

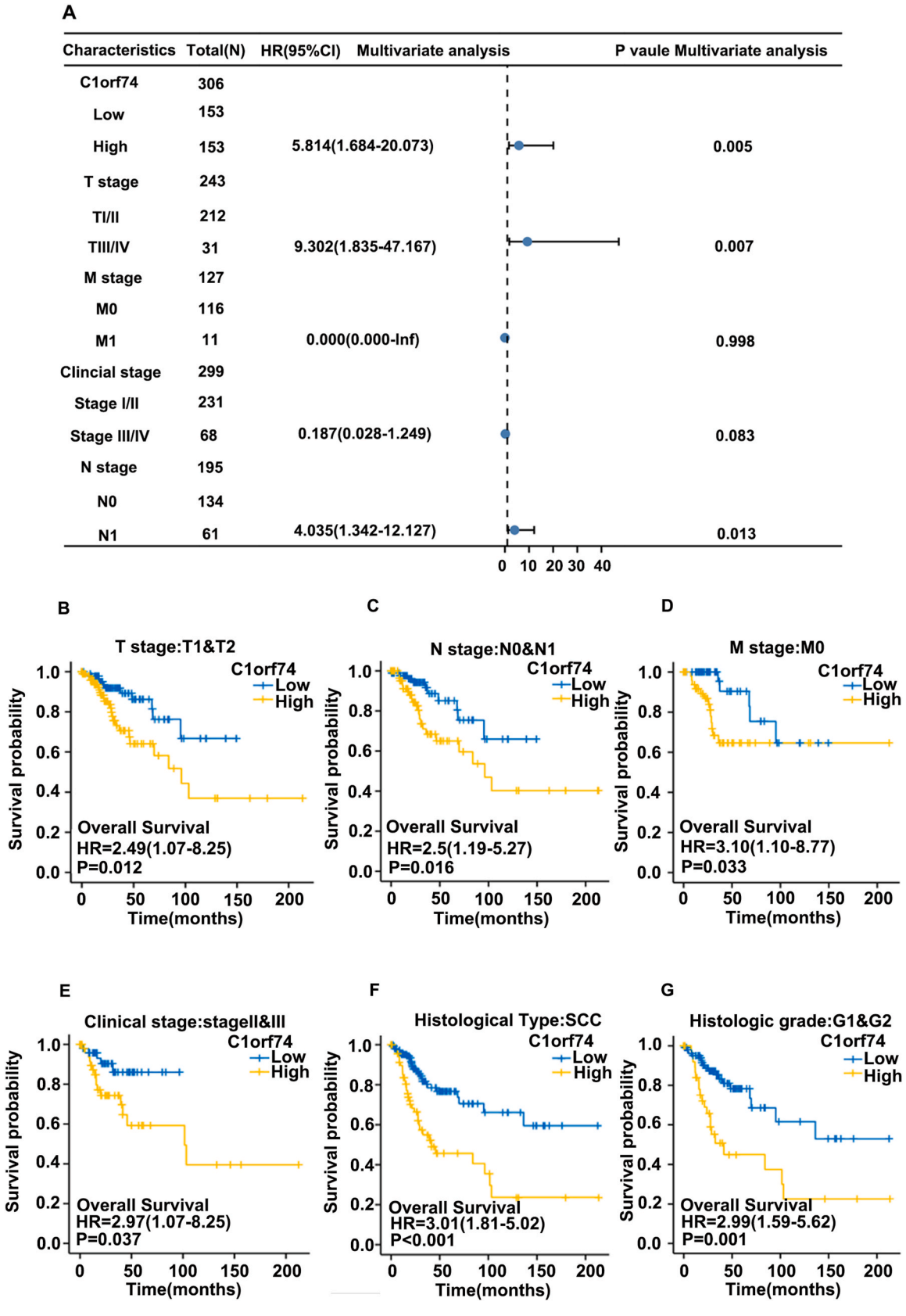

(caption on next page)

Fig. 5. Prognostic values of C1orf74 expression in patients with cervical cancer. **(A)** Forest map based on multivariate Cox analysis for overall survival. **(B–G)** OS survival curves of T1 and T2, N0 and N1, M0, stage II and III, SCC, G1 and G2 subgroups between high- and low-C1orf74 patients with cervical cancer. HR, hazard ratio; CI, confidence interval. OS, overall survival; T, T stage; N, N stage; M, M stage; SCC, squamous cell carcinoma; G, Grade.

and G2 (Fig. 5B–G).

To ascertain prognostic factors, both univariate and multivariate Cox regression analyses were performed, as illustrated in Figs. 4C and 5A. The multivariate analysis identified C1orf74 expression (HR = 5.814, 95 % CI = 1.684–20.073, p = 0.005), T stage (HR = 9.302, 95 % CI = 1.835–47.167, p = 0.007), and N stage (HR = 4.035, 95 % CI = 1.342–12.127, p = 0.013) as independent prognostic factors for overall survival (OS) in patients with cervical cancer, as shown in Fig. 5A and detailed in Table 3.

3.4. Construction and validation of a nomogram

In order to forecast the prognosis of individuals diagnosed with cervical cancer, a nomogram was constructed using independent factors associated with overall survival (OS). The graphical representation indicates that a higher cumulative score correlates with a poorer prognosis (Fig. 6A). Additionally, calibration curves were employed to evaluate the predictive performance of the nomogram (Fig. 6B–D). The bootstrap-adjusted concordance index (C-index) for the nomogram was 0.897 (95 % CI = 0.844–0.950). This indicates that the model has a moderate level of predictive accuracy for OS in cervical cancer patients. These findings collectively suggest the nomogram's applicability in clinical settings.

3.5. The top ten DEGs analysis

Based on the median of C1orf74 expression, patients with cervical cancer in TCGA were divided into high and low C1orf74 expression groups. Differentially expressed analysis of genes (DEGs) between these two groups was conducted using the R package DESeq2 (4), with adjusted $p < 0.05$, and $|\log_2 FC| > 3$ as the thresholds for identifying DEGs (Fig. 7A). We then assessed the correlation between the expression of the top ten most significantly DEGs and C1orf74 using Spearman's correlation analysis (Fig. 7B).

Table 3
Cox's proportional hazard model analysis of prognostic factors in patients with cervical cancer in TCGA.

Characteristics	Univariate			Multivariate		
	HR	95 % CI	p Value	HR	95 % CI	p Value
Clinical stage						
Stage I						
Stage II (II vs I)	0.813	0.413–1.601	0.550			
Stage III (III vs I)	1.275	0.632–2.570	0.498			
Stage IV (IV vs I)	4.446	2.392–8.263	**<0.001*****	0.187	0.028–1.249	0.083
Histologic grade						
G1						
G2 (G2 vs G1)	1.883	0.452–7.842	0.385			
G3 (G3 vs G1)	1.633	0.383–6.961	0.508			
G4 (G4 vs G1)	0.000	0.000-Inf	0.996			
Age (>50 vs ≤50)	1.317	0.825–2.101	0.248			
T stage						
T2 (T2 vs T1)	1.159	0.566–2.375	0.687			
T3 (T3 vs T1)	2.377	0.972–5.816	0.058			
T4 (T4 vs T1)	8.109	3.424–19.200	**<0.001*****	9.302	1.835–47.167	**0.007****
N stage						
(N1 vs N0)	2.695	1.358–5.349	**0.005****	4.035	1.342–12.127	**0.013***
M stage						
M1 (M1 vs M0)	3.646	1.220–10.892	**0.021***	0.000	0.000-Inf	0.998
Radiation therapy						
No						
Yes (Yes vs No)	1.153	0.681–1.951	0.596			
Race						
White (White vs Others)	1.189	0.603–2.344	0.618			
Histological type						
SCC (SCC vs AD)	1.010	0.530–1.926	0.976			
C1orf74						
High (High vs Low)	1.797	1.103–2.927	**0.019***	5.814	1.684–20.073	**0.005****

T: T stage; N0: No lymph node metastasis; N1: Lymph node metastasis; M0: No distant metastasis; M1: Distant metastasis; G: Histologic grade; KSCCP: Keratinizing squamous cell carcinoma present; SCC: Squamous Cell Carcinoma; AD: Adenosquamous; G: Histologic grade; KSCCP: keratinizing squamous cell carcinoma present; (*, $P < 0.05$; **, $P < 0.01$.).

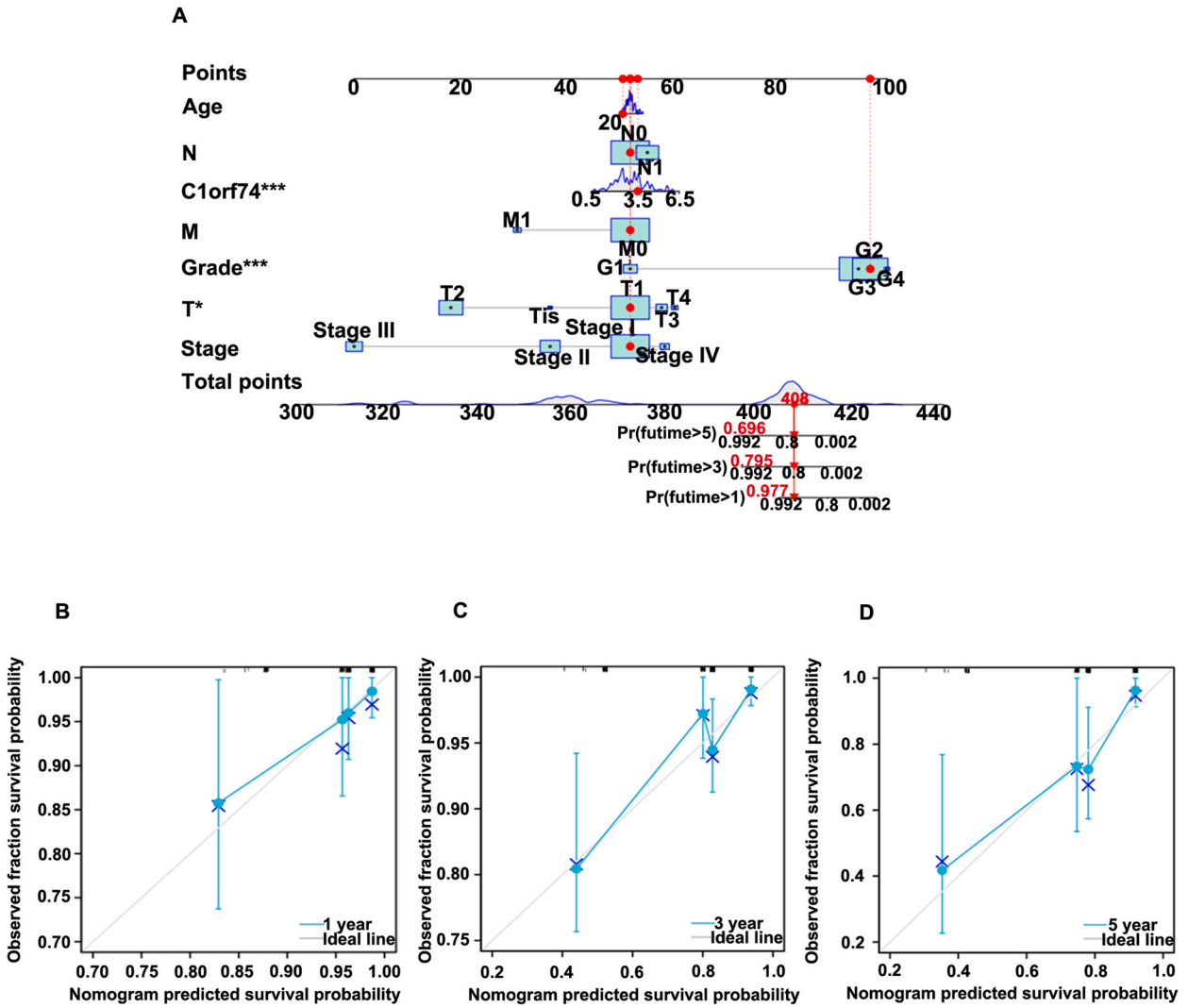

Fig. 6. A nomogram and calibration curves for prediction of one-, three-, and five-year overall survival rates of patients with cervical cancer. **(A)** A nomogram for prediction of one-, three-, and five-year overall survival rates of patients with cervical cancer. **(B–D)** Calibration curves of the nomogram prediction of one-, three-, and five-year overall survival rates of patients with cervical cancer. *, $p < 0.05$; ***, $p < 0.001$.

3.6. Functional enrichment analysis

Gene Ontology (GO) enrichment analysis, encompassing biological processes, cellular components, and molecular functions, indicated that DEGs were significantly associated with various GO terms, including antimicrobial humoral response, ciliary movement, the determination of bilateral symmetry, and digestive processes (Fig. 7C). Furthermore, the Kyoto Encyclopedia of Genes and Genomes (KEGG) pathway identified pathways that were enriched with DEGs, notably including chemical carcinogenesis, gastric cancer development, and melanoma formation (Fig. 7D). Subsequently, Gene Set Enrichment Analysis (GSEA) was conducted to compare the high and low expression groups of C1orf74, revealing a significant enrichment of the MAPK signaling pathway in the low C1orf74 expression cohort. This finding implies that the elevated levels of C1orf74 may facilitate the progression of cervical cancer (Fig. 7E).

3.7. Correlation between C1orf74 expression and immune infiltration

The distribution of 22 distinct types of immune lymphocytes within the tumor microenvironment (TME) of uterine corpus endometrial carcinoma (UCEC) was assessed using the CIBERSORT algorithm, as illustrated in Fig. 8A. Notably, the expression levels of C1orf74 exhibited a significant negative correlation with the infiltration of various immune cell types, including CD8+T cells ($p < 0.001$), naive B cells ($p = 0.003$), and mast cells ($p = 0.035$). Furthermore, within the group characterized by high expression of C1orf74, the quantities of CD8+T cells, M0 macrophages, activated dendritic cells, activated mast cells, and neutrophils were

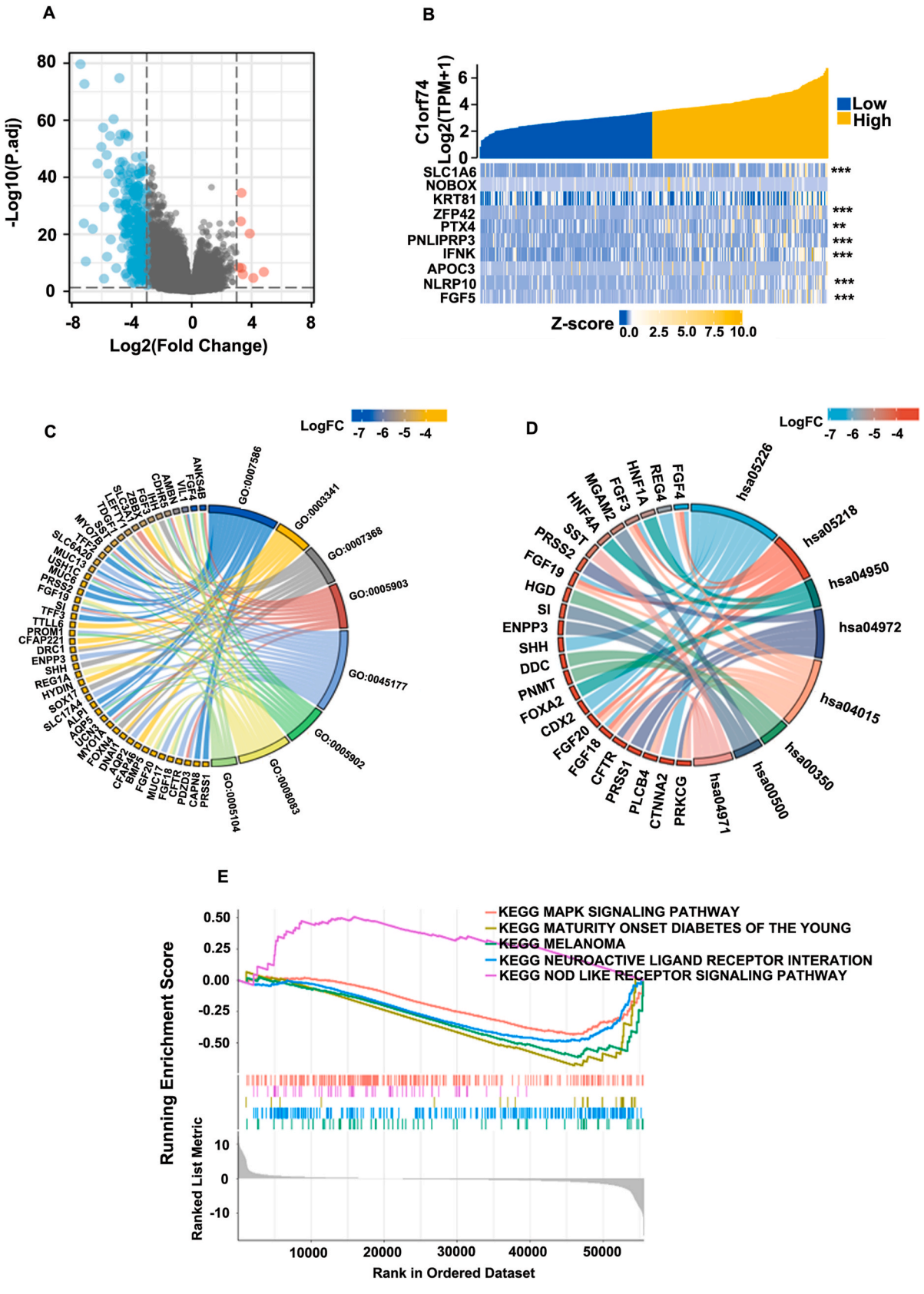

(caption on next page)

Fig. 7. C1orf74-related differentially expressed genes (DEGs) and functional enrichment analysis of C1orf74 in cervical cancer using GO, KEGG and GSEA. **(A)** Volcano plot of DEGs. Blue and red dots indicate the significantly down-regulated and up-regulated DEGs, respectively. **(B)** Heatmap of correlation between C1orf74 expression and the top 10 DEGs. **(C)** GO analysis of DEGs. **(D)** KEGG analysis of DEGs. **(E)** GSEA analysis of DEGs. GO, Gene Ontology; KEGG, Kyoto Encyclopedia of Genes and Genomes; DEGs, differentially expressed genes. GSEA, Gene Set Enrichment Analysis; **, $p < 0.01$, and ***, $p < 0.001$.

significantly diminished compared to those in the low expression group of C1orf74 (all $p < 0.05$), as shown in Fig. 8B. Additionally, an analysis was conducted to explore the correlations between the relative enrichment scores of immune cells and the expression levels of C1orf74, as shown in Fig. 8C–I.

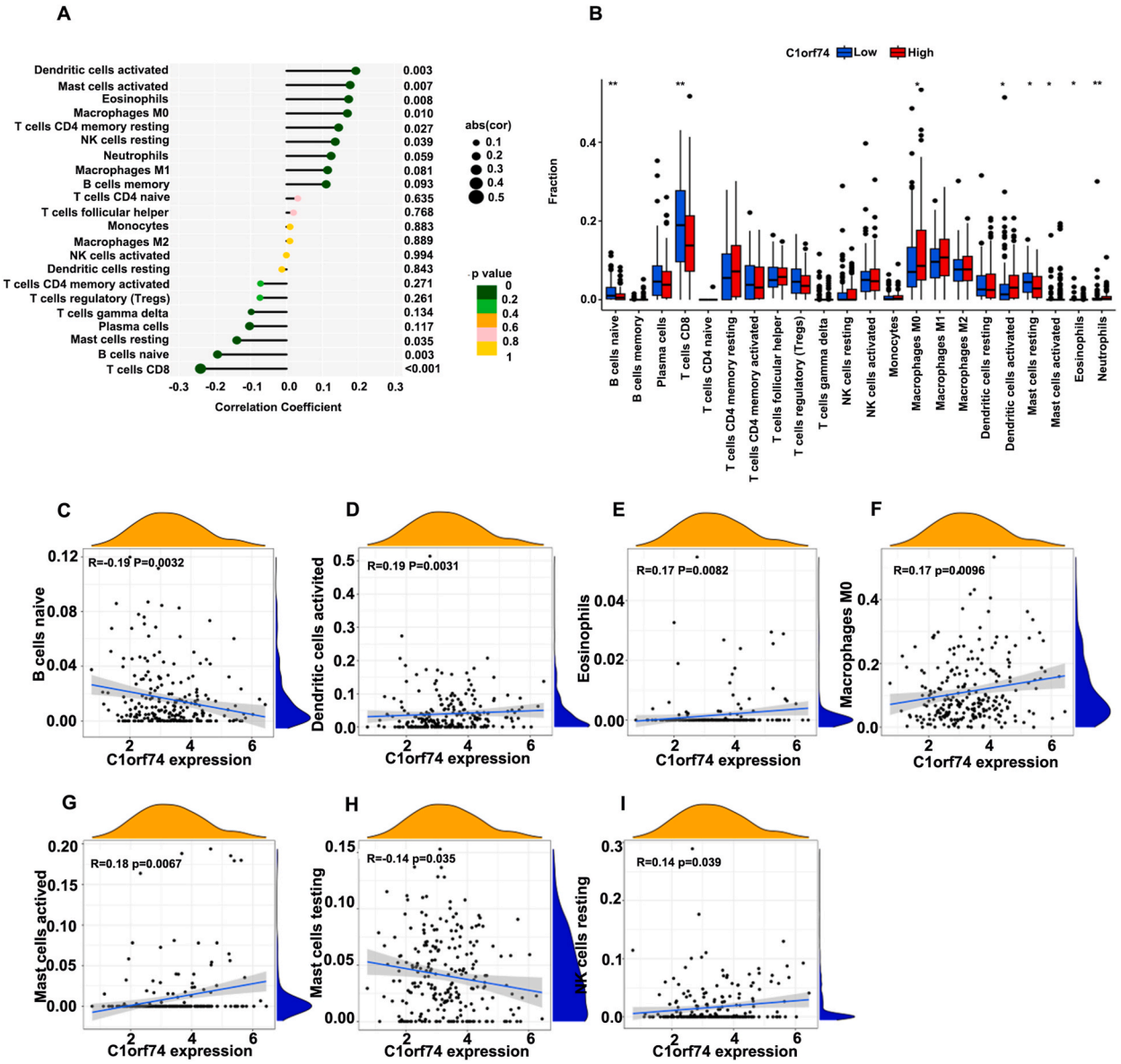

Fig. 8. Correlation of C1orf74 expression with immune infiltration level in cervical cancer. **(A)** Correlation between C1orf74 expression and relative abundance of 22 types of immune cell. The size of dot corresponds to the absolute Spearman's correlation coefficient values. **(B)** Comparison of immune infiltration levels of immune cells (including B cells naive cells, $CD8^{+}$T cells, M0 macrophages, dendritic cells activated, mast cells resting, mast cells activated, eosinophils, and neutrophils) between the high- and low-C1orf74 expression groups. **(C–I)** Correlations between the relative enrichment scores of immune cells (B cells, dendritic cells, eosinophils, M0 macrophage, mast cells, NK cells) and the expression of C1orf74. NK cells, natural killer cells.

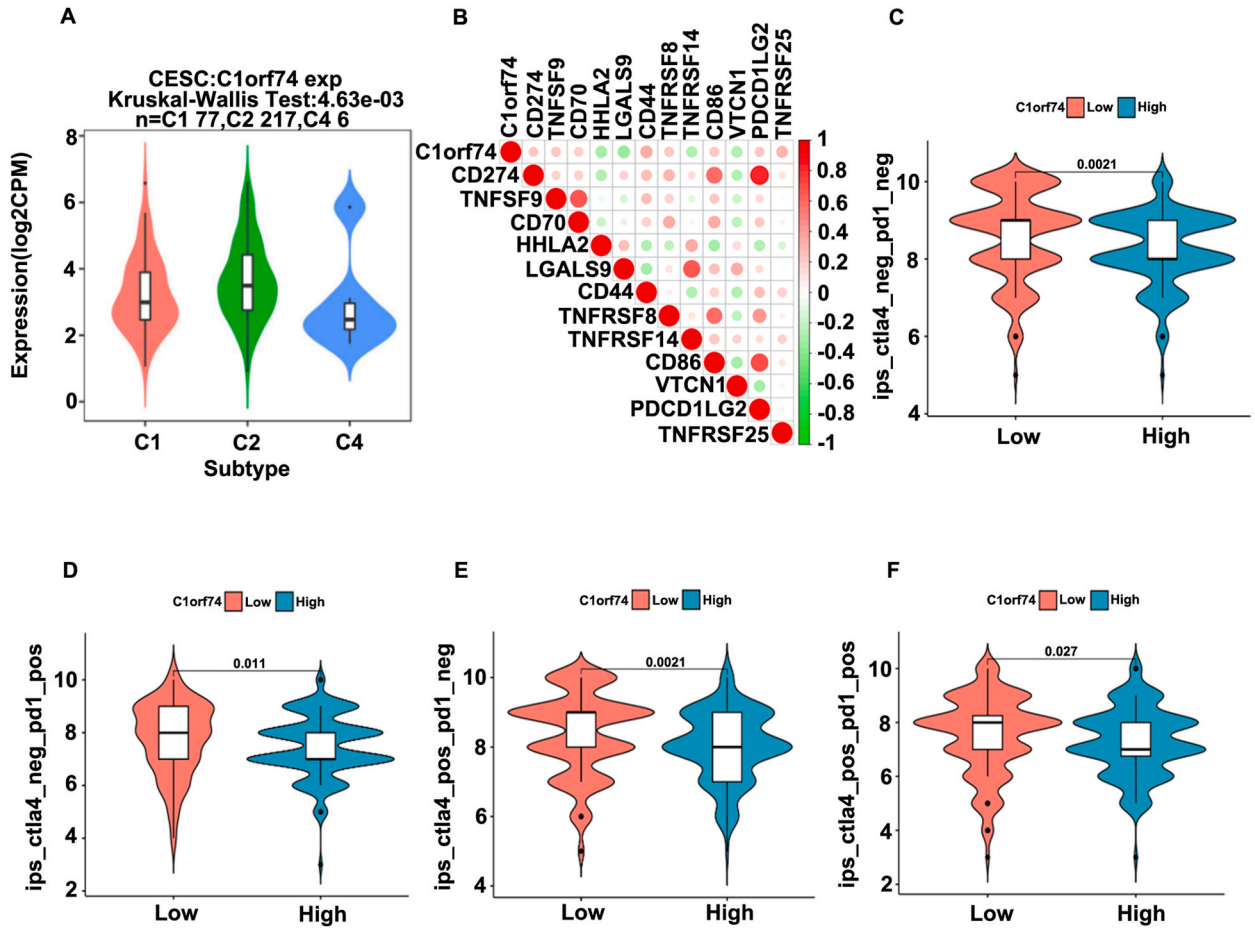

Fig. 9. Correlation analysis of C1orf74 to the immune checkpoint and IPS. **(A)** Correlations between C1orf74 expression and immune subtypes in cervical cancer. C1 (wound healing), C2 (IFN-g dominant), C3 (inflammatory). **(B)** The association gene with C1orf74 in cervical cancer present as heatmap. **(C)** The IPS. **(D)** IPS-PD-1/PD-L1/PD-L2. **(E)** IPS-CTLA4, and (F) IPS-PD-1/PD-L1/PD-L2 + CTLA4.

3.8. Correlation between C1orf74 expression and immune checkpoints

The TISIDB comprehensive repository (accessible at http://cis.hku.hk/TISIDB/index.php) serves as an online platform that aggregates data on cervical cancer derived from TCGA datasets. Utilizing the TISIDB database, we examined the expression levels of C1orf74 and its relationship with immune subtypes of cervical cancer. The findings, illustrated in Fig. 9A, indicate a significant correlation ($p < 0.05$) between the expression of C1orf74 and the immune subtypes associated with cervical cancer. Additionally, the genes associated with C1orf74 are presented in a heatmap (Fig. 9B). Given the observed positive correlation between the expression of C1orf74 and immune checkpoints, we further explored the relationship between immune checkpoint inhibitors (ICIs) and the expression of C1orf74. The IPS analysis revealed that patients exhibiting low levels of C1orf74 expression had a higher IPS score for anti-PD-1 and anti-CTLA4 immunotherapy, suggesting a potentially enhanced response to immunotherapy (Fig. 9C–F).

3.9. C1orf74 promoted the proliferation, migration and invasion abilities of cervical cells

We have done some biological experiments to explore the possible functions of C1orf74. The relative expression of C1orf74 in two cervical cancer cell line (SiHa, HeLa) was increased compared with the normal cervical cell line H8 (Fig. 10A). Subsequently, siRNAs (si-control group (si-nc), si-C1orf74) were transfected to SiHa and HeLa cells. QRT-PCR showed that C1orf74 expression was significantly downregulated in both cell lines transfected with si-C1orf74 compared with that transfected with si-nc (Fig. 10B). Furthermore, results from the CCK-8 assay showed that the ability of proliferation was reduced in SiHa and HeLa cells with knockdown of C1orf74 (si-C1orf74) than the control group (Fig. 10C–D). The colony formation assay showed that the number of colonies was decreased in the si-c1orf74 group compared with the si-nc (Fig. 10E–F). Next, analysis from the wound healing assay analysis indicated that knockdown of C1orf74 attenuated SiHa and HeLa cells migration (Fig. 10G–I). Transwell assay indicated that knockdown C1orf74 reduced cell migration and invasion abilities (Fig. 10J–K). These results showed that C1orf74 might promote SiHa and HeLa cells proliferation, migration and invasion, suggesting that C1orf74 played a critical role in promoting progression of cervical cancer.

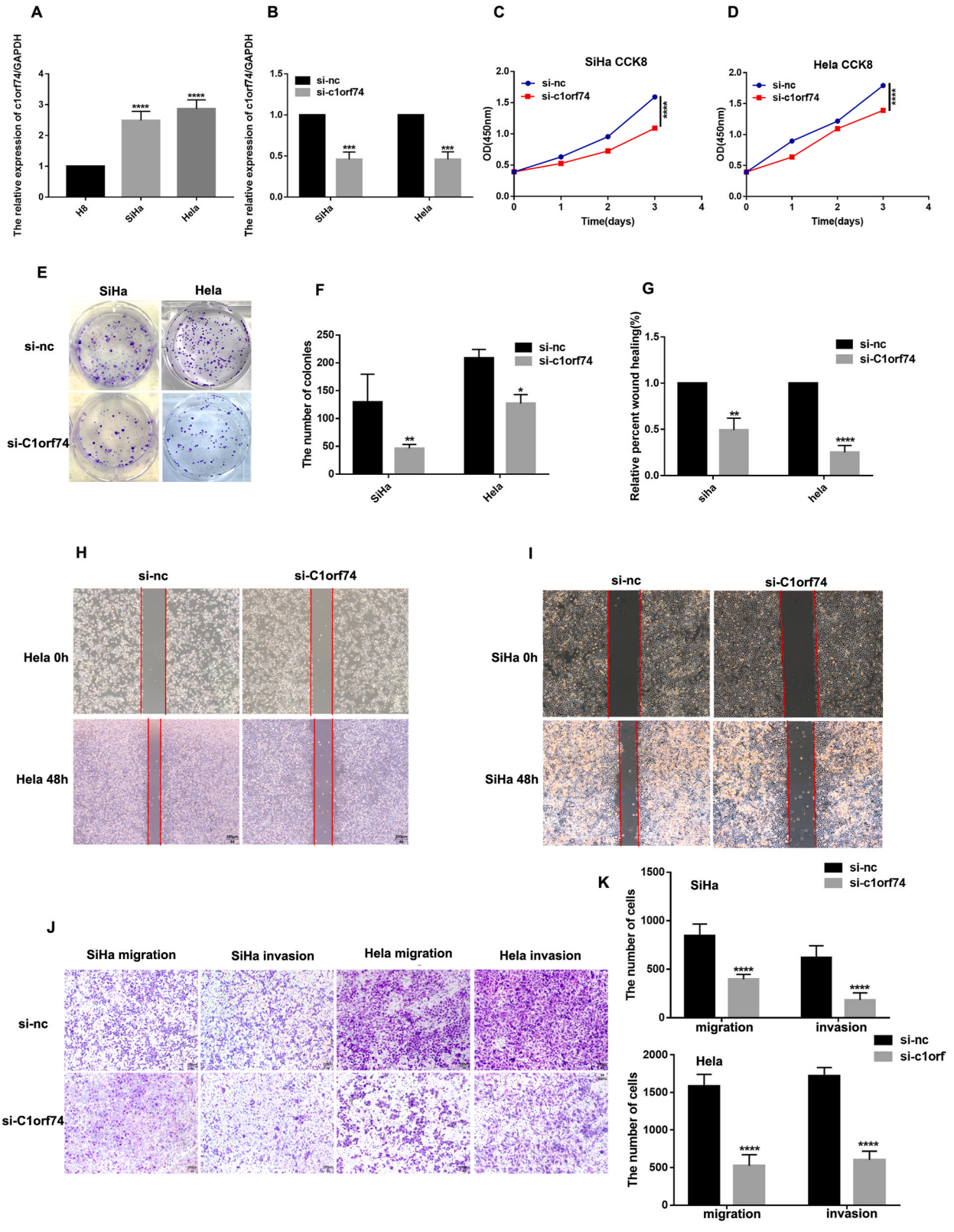

(caption on next page)

Fig. 10. C1orf74 promotes proliferation, migration and invasion of CC. **(A)** The expression of C1orf74 in cervical cancer cells (SiHa and HeLa) and the normal cervical cell (H8) by qRT-PCR. **(B)** Expression of C1orf74 in SiHa and HeLa cells transfection efficiency detection by qRT-PCR. **(C)** and **(D)** SiHa and HeLa cells were transfected with si-C1orf74 by the CCK-8 assay. **(E)** and **(F)** SiHa and HeLa cells were transfected with si-C1orf74 by the colony assay. **(G–I)** SiHa and HeLa cells were transfected with si-C1orf74 by the wound healing assay. **(J–K)** SiHa and HeLa cells were transfected with si-C1orf74 by transwell assay. *, $p < 0.05$; **, $p < 0.01$; ***, $p < 0.001$; and****, $p < 0.0001$.

4. Discussion

Cervical cancer ranks as the fourth most prevalent cancer globally and stands as a significant contributor to cancer-related mortality among women, with an estimated 570,000 new diagnoses and 311,000 fatalities each year [23]. The five-year survival rate is significantly lower for patients diagnosed with advanced stages of cervical cancer [24]. Thus, finding new molecular biomarkers is essential for improving the prognosis of CC patients. In this study, we first analyzed the expression level of C1orf74 in pan-cancerous tissues and found that C1orf74 was significantly upregulated in the majority of tumor tissues, including CC, compared with non-tumor tissues. C1orf74 is a protein found in the cytoplasm and cytoplasmic membrane [25]. Increased expression of C1orf74 has also been observed in lung adenocarcinoma [5]. However, its role in CC is still unknown.

Using a publicly available dataset, our analysis showed a significant correlation between C1orf74 expression levels and various clinical parameters, including clinical stage, T stage, and histological type in CC. This finding highlights the need for better monitoring or the start of adjuvant therapy for patients with high C1orf74 expression, as they are at a greater risk for recurrence. Furthermore, we evaluated the prognostic significance of C1orf74 in relation to OS in individuals diagnosed with CC. Our results showed that patients with high C1orf74 expression had a worse prognosis than those with lower expression levels. In summary, C1orf74 expression serves as a risk factor in CC. Moreover, our findings suggest that higher C1orf74 expression could serve as an independent prognostic biomarker for poor OS and DSS in CC patients. Consistent with our results, prior research has indicated that C1orf74 expression may serve as a prognostic marker for reduced survival rates in lung adenocarcinoma patients [5]. The findings indicate that C1orf74 is a promising target for effective cancer treatments.

Tumor cells grow in a microenvironment made up of cancerous cells, immune cells, and stromal cells [26]. Malignant tumor cells, like those in CC, are usually surrounded by immune cells that infiltrate the tumor microenvironment [27]. The prognostic significance of tumor-infiltrating immune cells in solid tumors is well recognized. Their impact is influenced by factors such as the type, density, and spatial distribution of these immune cells [28]. Additionally, infiltrating immune cells can predict responses to both neoadjuvant chemotherapy and immune checkpoint inhibition (ICI) therapy [29]. Therefore, assessing immune cell infiltration in cervical cancer may serve both complement ICI combination therapy and significantly predict ICI treatment outcomes. We examined the relationship between C1orf74 expression and the infiltration of various immune cells, revealing that higher C1orf74 expression negatively correlation with the infiltration levels of CD8+T cells, naive B cells, and mast cells. Activated CD8+T cells, B cells, and mast cells, which are components of the innate immune response, have been shown to suppress the proliferation of CC cells. Furthermore, the presence of CD8+T cells has been linked to enhanced prognostic outcomes in patients with CC. These findings suggest that C1orf74 overexpression may affect the progression and prognosis of CC by altering immune cell infiltration levels.

Based on these findings, we conducted functional loss assays to evaluate the biological behaviors associated with C1orf74. Our results indicate that C1orf74 significantly reduces proliferation, migration, and invasion of cells in vitro. To further substantiate these observations, we explored its potential mechanisms through bioinformatics analyses. The Gene Ontology, Kyoto Encyclopedia of Genes and Genomes pathway, and Gene Set Enrichment Analysis indicated that pathways enriched with DEGs were significantly affected. Notably, the MAPK signaling pathway was enriched in the group with decreased expression of C1orf74. These findings provide preliminary evidence that the knocking out C1orf74 inhibits the proliferation, migration, and invasion of CC cells by modulating the MAPK signaling pathway.

In summary, our research shows that C1orf74 expression is significantly higher in CC and closely linked to clinical staging and histological classification. Moreover, C1orf74 is a risk factor for poor prognoses and can promote the progression of CC in vitro. These findings suggest that C1orf74 as a potential biomarker for personalized therapeutic approaches, although further investigation into its cancer-promoting mechanisms is needed.

CRediT authorship contribution statement

Hai Zhu: Writing – original draft, Visualization, Validation, Software. **Yaping Wang:** Software, Methodology. **Yu Zhang:** Visualization, Software, Resources. **Yun Tian:** Investigation, Data curation. **Duan Liu:** Investigation, Data curation. **Xiabing Li:** Validation, Methodology. **Gaili Ji:** Validation, Data curation. **Caixia Ma:** Writing – review & editing. **Hongyu Li:** Writing – review & editing, Resources, Funding acquisition.

Patient consent for publication

Not applicable.

Ethics approval and consent to participate

The study approved by the Ethics Committee of the Third Affiliated Hospital of Zhengzhou University. Protocol number:2024-362-01.

Funding

This study was supported in part by grants from the National Natural Science Foundation of China (82272332) and by grants from Joint Project of Henan Medical Science and Technology Research Plan of china (SBGJ202002091).

Declaration of competing interest

The authors declare that they have no known competing financial interests or personal relationships that could have appeared to influence the work reported in this paper.

Acknowledgments

Not applicable.

References

[1] J. Park, J. Lee, Y. Lee, S. Shim, D. Suh, J. Kim, Major clinical research advances in gynecologic cancer in 2021, J. Gynecol. Oncol. 33 (2) (2022) e43.
[2] Erratum, Global cancer statistics 2018: GLOBOCAN estimates of incidence and mortality worldwide for 36 cancers in 185 countries, CA Cancer J. Clin. 70 (4) (2020) 313.
[3] P. Hass, H. Eggemann, S.D. Costa, A. Ignatov, Adjuvant hysterectomy after radiochemotherapy for locally advanced cervical cancer, Strahlenther. Onkol. 193 (12) (2017) 1048–1055.
[4] H. van Meir, G.G. Kenter, J. Burggraaf, J.R. Kroep, M.J. Welters, C.J. Melief, et al., The need for improvement of the treatment of advanced and metastatic cervical cancer, the rationale for combined chemo-immunotherapy, Anti Cancer Agents Med. Chem. 14 (2) (2014) 190–203.
[5] J. Guo, A. Li, R. Guo, Q. He, Y. Wu, Y. Gou, et al., C1orf74 positively regulates the EGFR/AKT/mTORC1 signaling in lung adenocarcinoma cells, PeerJ 10 (2022) e13908.
[6] W. Wang, C. Zhang, H. Liu, C. Xu, H. Duan, X. Tian, et al., Heritability and genome-wide association analyses of fasting plasma glucose in Chinese adult twins, BMC Genom. 21 (1) (2020) 491.
[7] X. Guo, S. Chen, S. Wang, H. Zhang, F. Yin, P. Guo, et al., CircRNA-based cervical cancer prognosis model, immunological validation and drug prediction, Curr. Oncol. 29 (11) (2022) 7994–8018.
[8] E. Cerami, J. Gao, U. Dogrusoz, B.E. Gross, S.O. Sumer, B.A. Aksoy, The cBio cancer genomics portal: an open platform for exploring multidimensional cancer genomics data (vol 2, pg 401, 2012), Cancer Discov. 2 (5) (2012) 401–404.
[9] Y.L. Ahmed, S. Schleich, J. Bohlen, N. Mandel, B. Simon, I. Sinning, et al., DENR-MCTS1 heterodimerization and tRNA recruitment are required for translation reinitiation, PLoS Biol. 16 (6) (2018).
[10] K. Asada, K. Miyamoto, T. Fukutomi, H. Tsuda, Y. Yagi, K. Wakazono, et al., Reduced expression of and silencing of in human breast cancers, Oncology-Basel 64 (4) (2003) 380–388.
[11] M. Deng, C. Xiong, Z.K. He, Q. Bin, J.Z. Song, W. Li, et al., As a novel prognostic biomarker and its correlation with immune infiltrates in breast cancer, Front. Genet. 13 (2022).
[12] S. Liu, L. Song, H. Yao, L. Zhang, HPV16 E6/E7 stabilize PGK1 protein by reducing its poly-ubiquitination in cervical cancer, Cell Biol. Int. 46 (3) (2022) 370–380.
[13] Y.F. Zheng, P. Jiang, Y. Tu, Y.Z. Huang, J.Y. Wang, S.K. Gou, et al., Incidence, risk factors, and a prognostic nomogram for distant metastasis in endometrial cancer: a SEER-based study, Int. J. Gynecol. Obstet. 165 (2) (2024) 655–665.
[14] M. Gönen, G. Heller, Concordance probability and discriminatory power in proportional hazards regression, Biometrika 92 (4) (2005) 965–970.
[15] W. Walter, F. Sanchez-Cabo, M. Ricote, GOplot: an R package for visually combining expression data with functional analysis, Bioinformatics 31 (17) (2015) 2912–2914.
[16] A. Subramanian, P. Tamayo, V.K. Mootha, S. Mukherjee, B.L. Ebert, M.A. Gillette, et al., Gene set enrichment analysis: a knowledge-based approach for interpreting genome-wide expression profiles, Proc. Natl. Acad. Sci. U. S. A. 102 (43) (2005) 15545–15550.
[17] Z. Nie, T. Pu, Z.J. Han, C.Y. Wang, C.L. Pan, P. Li, et al., Extra spindle Pole bodies-like 1 serves as a prognostic biomarker and promotes lung adenocarcinoma metastasis, Front. Oncol. 12 (2022).
[18] P. Charoentong, F. Finotello, M. Angelova, C. Mayer, M. Efremova, D. Rieder, et al., Pan-cancer immunogenomic analyses reveal genotype-immunophenotype relationships and predictors of response to checkpoint blockade, Cell Rep. 18 (1) (2017) 248–262.
[19] P. Jiang, S. Gu, D. Pan, J. Fu, A. Sahu, X. Hu, et al., Signatures of T cell dysfunction and exclusion predict cancer immunotherapy response, Nat. Med. 24 (10) (2018) 1550–1558.
[20] C. Paules, A.P. Dantas, J. Miranda, F. Crovetto, E. Eixarch, V. Rodriguez-Sureda, et al., Premature placental aging in term small-for-gestational-age and growth-restricted fetuses, Ultrasound Obstet. Gynecol. 53 (5) (2019) 615–622.
[21] Y. Shiraishi, K. Kryukov, K. Tomomatsu, F. Sakamaki, S. Inoue, S. Nakagawa, et al., Diagnosis of pleural empyema/parapneumonic effusion by next-generation sequencing, Infect. Dis. 53 (6) (2021) 450–459.
[22] J.L. Sepulveda, Using R and bioconductor in clinical genomics and transcriptomics, J. Mol. Diagn. 22 (1) (2020) 3–20.
[23] S.S. Cohen, R.T. Palmieri, S.J. Nyante, D.O. Koralek, S. Kim, P. Bradshaw, et al., Obesity and screening for breast, cervical, and colorectal cancer in women: a review, Cancer 112 (9) (2008) 1892–1904.
[24] J.D. Wright, K. Matsuo, Y. Huang, A.I. Tergas, J.Y. Hou, F. Khoury-Collado, et al., Prognostic performance of the 2018 international federation of gynecology and obstetrics cervical cancer staging guidelines, Obstet. Gynecol. 134 (1) (2019) 49–57.
[25] M. Uhlen, L. Fagerberg, B.M. Hallstrom, C. Lindskog, P. Oksvold, A. Mardinoglu, et al., Proteomics. Tissue-based map of the human proteome, Science 347 (6220) (2015) 1260419.
[26] L. Ferrall, K.Y. Lin, R.B.S. Roden, C.F. Hung, T.C. Wu, Cervical cancer immunotherapy: facts and hopes, Clin. Cancer Res. 27 (18) (2021) 4953–4973.

[27] M.S. Pfaffenzeller, M.L.M. Franciosi, A.M. Cardoso, Purinergic signaling and tumor microenvironment in cervical Cancer, Purinergic Signal. 16 (1) (2020) 123–135.
[28] Y. Li, X. Gao, Y. Huang, X. Zhu, Y. Chen, L. Xue, et al., Tumor microenvironment promotes lymphatic metastasis of cervical cancer: its mechanisms and clinical implications, Front. Oncol. 13 (2023) 1114042.
[29] J.J. Havel, D. Chowell, T.A. Chan, The evolving landscape of biomarkers for checkpoint inhibitor immunotherapy, Nat. Rev. Cancer 19 (3) (2019) 133–150.